1-2013

Single-cell Imaging And Spectroscopic Analyses Of Cr(vi) Reduction On The Surface Of Bacterial Cells

Yuanmin Wang

Papatya C. Sevinc

Sara M. Belchik

Jim Fredrickson

Liang Shi

See next page for additional authors

Langmuir

Article

pubs.acs.org/Langmuir

Single-Cell Imaging and Spectroscopic Analyses of Cr(VI) Reduction on the Surface of Bacterial Cells

Yuanmin Wang,[†] Papatya C. Sevinc,[†] Sara M. Belchik,[‡] Jim Fredrickson,[‡] Liang Shi,[‡] and H. Peter Lu*[,†]

[†]Department of Chemistry, Center for Photochemical Sciences, Bowling Green State University, Bowling Green, Ohio 43403, United States

[‡]Microbiology Group, Biological Sciences Division, Pacific Northwest National Laboratory, Richland, Washington 99352, United States

Supporting Information

ABSTRACT: We investigate the single-cell reduction of toxic Cr(VI) by the dissimilatory metal-reducing bacterium *Shewanella oneidensis* MR-1 (MR-1), an important bioremediation process, using Raman spectroscopy and scanning electron microscopy (SEM) combined with energy-dispersive X-ray spectroscopy (EDX). Our experiments indicate that the toxic, highly soluble Cr(VI) can be efficiently reduced to less toxic, nonsoluble Cr_2O_3 nanoparticles by MR-1. Cr_2O_3 is observed to emerge as nanoparticles adsorbed on the cell surface and its chemical nature is identified by EDX imaging and Raman spectroscopy. Co-localization of Cr_2O_3 and cytochromes by EDX imaging and Raman spectroscopy suggests a terminal reductase role for MR-1 surface-exposed cytochromes MtrC and OmcA. Our experiments revealed that the cooperation of surface proteins OmcA and MtrC makes the reduction reaction most efficient, and the sequence of the reducing reactivity of MR-1 is wild type > single mutant Δ*mtrC* or mutant Δ*omcA* > double mutant (Δ*omcA*−Δ*mtrC*). Moreover, our results also suggest that direct microbial Cr(VI) reduction and Fe(II) (hematite)-mediated Cr(VI) reduction mechanisms may coexist in the reduction processes.

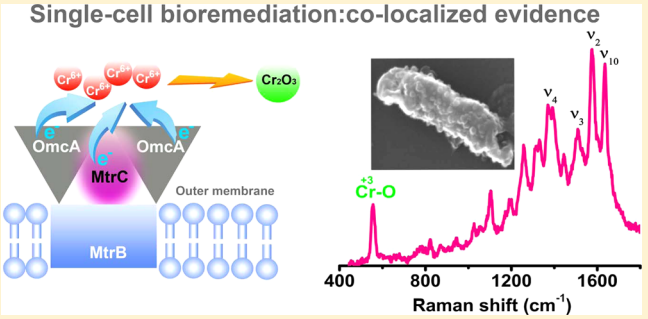

INTRODUCTION

Hexavalent chromium [Cr(VI)] contamination of the soil and groundwater is a significant environmental hazard that has attracted considerable attention in the scientific community.[1,2] For a human being, Cr(VI) toxicity can lead to many health impacts such as carcinogenesis and mutagenesis.[3] Because of its high aqueous solubility and mobility, Cr(VI) contamination can be proliferated to spread to a vast area through groundwater. Therefore, reducing highly soluble, toxic Cr(VI) to less-soluble, less-toxic Cr(III) in the form of Cr_2O_3 precipitates is the primary strategy for contamination treatment.

In a natural environment, direct microbial reduction and chemical reaction using Fe^{2+} or S^{2-} as a reductant are two typical approaches to decrease the Cr(VI) contamination. Microbial reduction has been widely utilized in bioremediation approaches to the environmental cleanup of Cr(VI) contamination in the soil because it is a feasible and promising strategy considering that bacteria naturally exist and pervade a wide area even underground and under anaerobic conditions. In recent years, many bacteria have been demonstrated to have the capability to reduce Cr(VI) to Cr(III).[4−9] As a dissimilatory metal-reducing bacterium, *Shewanella oneidensis* MR-1 (MR-1) has also been reported to be capable of reducing Cr(VI), and the reduced product has been shown to occur as nanoparticles on the bacterial cell surface or in the cytoplasm, including our recent report on the reduction activities of outer membrane proteins on reducing Cr(VI).[3,6,10−14]

Raman spectroscopy is a unique technique, giving fingerprint information about the molecules (such as proteins and organics) to identify various molecules and probe specific vibrational modes that are sensitive to the redox states of the molecules.[15,16] Recently, we have applied high-resolution AFM-Raman spectroscopy to probe the chemical nature of the cell surface nanodomains (i.e., the surface features on the nanometer scale) of MR-1.[17] It is demonstrated that the distribution density of the nanodomains shows clear differences under aerobic and anaerobic conditions and that the major component of the cell surface domains is identified to be the redox heme proteins. This finding may help to reveal the mechanism of the Cr(VI) reduction by MR-1. Moreover, surface heme proteins OmcA and MtrC (also known as OmcB) of MR-1 have been proven to play a key role in the reduction of Fe(III), Mn(III/IV), and Cr(VI).[10,18−22] In this report, we apply combined surface-enhanced Raman spectroscopy, SEM, and EDX imaging to probe the Cr(VI) reduction mechanism at the single-cell level. Our spectroscopic and imaging evidence

Received: July 14, 2012
Revised: December 11, 2012
Published: December 18, 2012

indicates the following: the chemical nature of the reduced nanoparticles is Cr_2O_3; co-localization of reduced Cr_2O_3, MtrC, and OmcA signifies that surface proteins OmcA and MtrC are the key components in the Cr(VI) reduction reaction; the cooperation of OmcA and MtrC makes the reduction reaction most efficient; and both direct Cr(VI) reduction by MtrC and OmcA and Fe(II)-mediated Cr(VI) reduction mechanisms in which Fe(II) is generated by MtrC and OmcA through Fe(III) reduction are suggested to coexist in the Cr(VI) reduction process.

EXPERIMENTAL SECTION

Materials and Sample Preparation. *S. oneidensis* MR-1 and its cytochrome-deleted mutants Δ*mtrC*, Δ*omcA*, and Δ*mtrC*−Δ*omcA*, are described in the previous study.[10] Wild-type *S. oneidensis* MR-1 and the various mutants used were routinely cultured at 30 °C in dextrose-free tryptic soy broth (TSB, Difco, Lawrence, KS). The Cr(VI) experiments were carried out by using a resting-cell assay. TSB cultures (50 mL) were grown aerobically for 16 h at 30 °C and 100 rpm and harvested by centrifugation at 5000*g* for 5 min. Under these conditions, no growth defect was observed for the mutants used. Cells were washed once in an equal volume of 30 mM sodium bicarbonate buffer (pH 8) at 4 °C. Following centrifugation, the cells were resuspended in the bicarbonate buffer at a density of 2×10^9 cells/mL and purged for 10 min with mixed CO_2/N_2 (80:20) gas. Cr(VI) reduction assays contained 30 mM sodium bicarbonate, pH 8, 0.2 mM K_2CrO_4 (Sigma, St. Louis, MO) and 10 mM sodium lactate that was purged with the mixed CO_2/N_2 gas and sealed with thick butyl rubber stoppers. Kinetic studies were initiated by adding the purged bacterial cells at a final density of 2×10^8 cells/mL. The same amount of heat-killed wild-type cells was added as a negative control. The reactions were carried out at 30 °C with horizontal incubation at 25 rpm. At predetermined time points, cells were harvested. After harvesting by centrifugation, bacterial cells were fixed in 2.5% glutaraldehyde.

For hematite reduction, the cells were prepared in the same way as described above. Hematite (11 ± 2 nm; sample received from Prof. Michael F. Hochella, Center for NanoBioEarth, Department of Geosciences, Virginia Tech) was added to a final concentration of 0.1 mM.[23] The reduction of hematite was carried out at 30 °C with horizontal incubation at 25 rpm.[31] At 24 h, K_2CrO_4 was added to a final concentration of 0.2 mM. The reductions were carried out under the condition described above. At predetermined time points, cells were harvested and fixed in the same way as described above.

Surface-Enhanced Raman Spectroscopy Measurements. SERS spectroscopy and imaging were conducted by using an Axiovert 135 inverted scanning confocal microscope equipped with a 100×, 1.3 NA oil-immersion objective (Zeiss FLUAR). A continuous-wave (CW) laser (532 nm, CrystaLaser) was used to pump the sample at 3 μW for SERS and 60 μW for resonance Raman measurements. A Z532rdc beam splitter (Chroma) was used to reflect the excitation light into the microscope objective. Before the scattered light is focused into a monochromator (Triax 550, Jobin Yvon), an HQ580/60 M band-pass filter or an HQ545 long-pass filter was positioned before the entrance slit to reject the Rayleigh light further. The Raman spectra were collected with an LN CCD (Princeton Instruments) cooled to about −100 °C with a resolution of 2 cm^{-1}. The setup was carefully calibrated using a mercury lamp and cyclohexane (mode at 801.3 cm^{-1}) before the Raman measurements were made. For the SERS experiments, we used Ag nanoparticles as the substrate, and the average size of the nanoparticles was about 50 nm (more details in Supporting Information).

SEM and EDX Imaging Measurements. About 3 μL of the glutaraldehyde-fixed cells was dropped onto a clean coverslip to make a dry film. The film was washed carefully with ultrapure water from Millipore. Once the sample dried, an electrically conductive thin carbon layer of nanometer thickness was used to coat the sample surface for an SEM imaging measurement. The SEM image was collected by using an FEI-Inspect F scanning electron microscope (FEI, Hillsboro, OR) with a spatial resolution of ∼1 nm. Secondary electrons were probed to obtain the SEM image at a typical acceleration voltage of 20 kV. An EDX system (INCA Penta FET × 3, Oxford Instruments, Abingdon, U.K.) was attached to the microscope to obtain the elements' (Cr and Fe) image.

RESULTS AND DISCUSSION

As outer membrane cytochromes (heme proteins), OmcA and MtrC have been suggested to be the major components showing the capability of extracellular respiration on the MR-1 surface.[18−22] We have further proven this attribution by our spectroscopic evidence (Figure 1) using resonance Raman

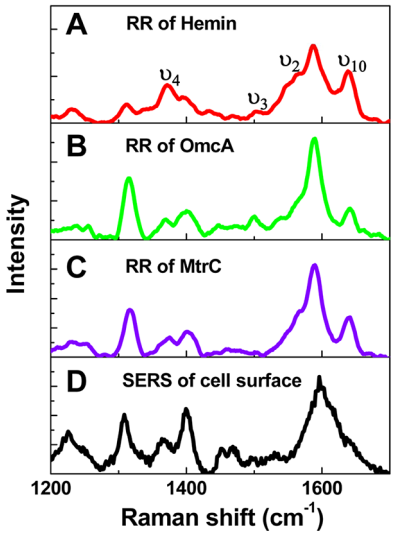

Figure 1. Resonance Raman spectra of hemin (A), OmcA (B), MtrC (C), and SERS of the cell outer surface of wild-type MR-1 (D). Although the Raman intensity shows fluctuations, typical vibrational modes such as ν_4, ν_3, ν_2, and ν_{10} are obvious. On the basis of the similarity of B, C, and D, proteins OmcA and MtrC are identified to be the main compositions of the outer membrane of MR-1, which is consistent with previous reports.[18]

(RR) spectroscopy and surface-enhanced Raman spectroscopy (SERS). Figure 1A−C shows the RR spectra of hemin chloride (an analogue of the heme group in c-type cytochrome), purified OmcA, and MtrC. The typical and signature vibrational modes of the heme group, such as ν_4, ν_3, ν_2, and ν_{10}, are clearly shown, and the spectral profiles are essentially the same among the examined samples, indicating that OmcA and MtrC are intrinsically heme proteins. Moreover, as the oxidation state marker, the mode ν_4 peak appears at 1373 cm^{-1}, implying that all three samples are in their oxidized states because of having a vibrational frequency in the range of ∼1368−1377 cm^{-1}, which pertains to the ferric (Fe^{III}) state.[24]

We have also applied SERS to investigate the chemical nature of the surface proteins of MR-1. As shown in Figure 1D, the Raman spectral profile of the wild-type cell surface matches the RR spectra of OmcA and MtrC, implying that the major components of the cell surface are dominated by *c*-type cytochrome. These spectroscopic identifications are consistent but beyond our previous measurements.[17,18] In addition, we note that the ν_4 mode in Figure 1D peaks at 1366 cm^{-1} unlike the RR of hemin, OmcA, and MtrC at 1373 cm^{-1}. The observed 7 cm^{-1} shift of the oxidation state marker is most likely due to the partial charge transfer between the cell surface

dx.doi.org/10.1021/la303779y | *Langmuir* 2013, 29, 950−956

heme proteins and the Ag substrate used for the SERS measurements.[25]

To check the reduction capability of the MR-1 cell surface, we performed a biological assay under anaerobic conditions by using Cr(VI) in solution. To prove the key roles of the surface proteins, OmcA and MtrC, in the reduction reaction, we have carried out four experiments under the same measurement conditions and assay protocol[10] on different MR-1 cells: (a) wild type, (b) Δ*mtrC* mutant, (c) Δ*omcA* mutant, and (d) Δ*mtrC*−Δ*omcA* double mutant. We applied SEM, EDX, and SERS to analyze the cell surfaces after Cr(VI) reduction. We have observed rough cell surfaces showing nanoparticles in the case of wild type, the Δ*mtrC* mutant, and the Δ*omcA* mutant but not for the double mutant Δ*mtrC*−Δ*omcA*. Because oxygen can be ruled out as an electron acceptor under anaerobic conditions, electron transfer from the cell surface to Cr(VI) is the only possible charge-transfer pathway. Therefore, the nanoparticles shown on the bacterial MR-1 cell surfaces are attributed to the reduced insoluble Cr(III) species (i.e., Cr_2O_3). As a typical case, we show the experimental data of the wild type MR-1 cells in Figure 2. From the SEM image (Figure 2A),

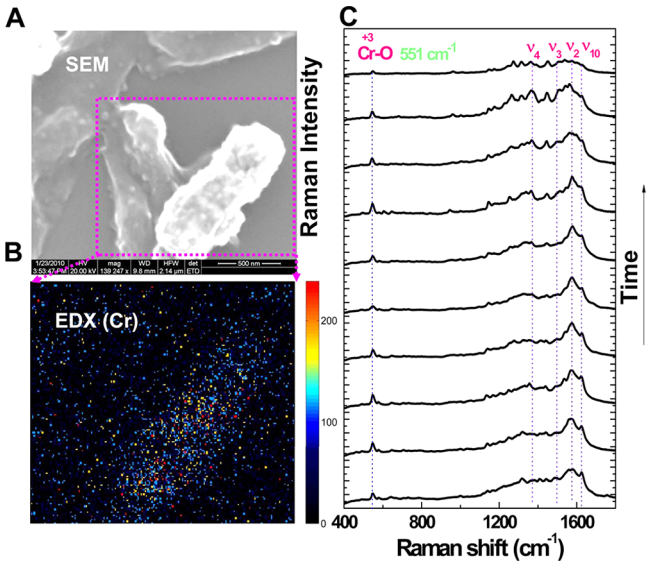

Figure 2. (A) Typical SEM image of MR-1 after the Cr(VI) reduction assay. (The scale bar for the SEM image is 500 nm.) Nanoparticles emerged on the cell surface after the reduction. An additional SEM image is shown in the Supporting Information to clearly show the nanoparticles on the cell surface. (B) Nanoparticles are suggested to be Cr by EDX characterization. (C) The chemical composition of the nanoparticles is identified to be the reduced product, Cr(III) (i.e., insoluble Cr_2O_3 by SERS depending on the occurring prominent peak at 551 cm^{-1}, the specific A_{1g} vibrational mode of the Cr(III)−O bond, and the typical peaks originating from the cell-surface proteins).

nanoparticles can be clearly observed. Figure 2B shows the EDX image of the two adjacent wild type cells in that only one of them is covered with a significant number of nanoparticles. Accordingly, a highly concentrated Cr element is observed on this cell surface. To probe the chemical nature of the formed nanoparticles further, we performed SERS measurements, and the results for wild type MR-1 are shown in Figure 2C. Obviously, besides the typical Raman vibrational modes (typical peaks from 1100 to 1650 cm^{-1}) originating from outer-membrane *c*-type cytochromes of MR-1, there is also an additional peak at 551 cm^{-1}, the A_{1g} vibrational mode of the Cr(III)−O bond that originated from Cr_2O_3. Other possible compounds, such as CrOOH and $Cr(OH)_3$, have different Raman shifts for their Cr(III)−O mode.[26,27] The co-localization of cytochromes and Cr(III) suggests that MtrC and OmcA reduce Cr(VI) directly, which is consistent with the terminal reductase roles of these cytochromes in Cr(VI) reduction.[10] On the basis of our control experiments, outer-membrane proteins OmcA and MtrC are demonstrated to be the dominant terminal reductases of the Cr(VI) reduction reaction. Combined with the statistical analysis of the density of the nanoparticles on all four samples as well as our recent discoveries,[10] we suggest that the reactivity of the reduction reaction changes in the order wild type > Δ*mtrC* mutant or Δ*omcA* mutant > Δ*omcA*−Δ*mtrC* double mutant. Our conclusion is consistent with the previous results.[10]

A fundamental understanding of the reduction mechanism of Cr(VI) is critical to the promotion of the bioremediation efficiency. Moreover, a clear and in-depth mechanism can also be used as a reference to study the bioremediation processes of other metal contaminants. Previously, the bioremediation mechanism of Cr(VI) has been suggested to be a direct microbial reduction[12,14] or an Fe(II)-mediated reduction[9,28,29] for the *Shewanella* species. Here, we demonstrate that these two mechanisms can coexist in the Cr(VI) reduction by MR-1.

Shewanella species have been observed to be capable of reductively transforming Fe(III) containing minerals such as ferrihydrite, goethite, and hematite (Fe_2O_3) in a natural, oxygen-limited environment.[30] Previously, electron exchange between the MR-1 and hematite nanoparticles has been suggested to occur by both direct and indirect mechanisms with the reduction rates altering according to the nanoparticle size, shape, and aggregation state.[31] Moreover, direct electron exchange between the surface proteins (OmcA and MtrC) of MR-1 and hematite associated Fe(II) electrodes has been demonstrated by using an electrochemical approach.[19] Because hematite is abundant on the earth, if it can mediate the reduction process between *Shewanella* and Cr(VI) it will aid natural Cr(VI) bioremediation. Therefore, our analytical assay for probing the Cr(VI) reduction mechanism was also performed with additional hematite. Figure 3 shows the imaging and spectroscopic characterizations of the hematite-involved Cr(VI) reduction by MR-1 cells. The SEM images (Figure 3A) show that a significant number of the nanoparticles appeared on the cell surfaces of wild type, the Δ*omcA* mutant, and the Δ*mtrC* mutant but not for Δ*omcA*−Δ*mtrC*. The additional 551 cm^{-1} Raman peak (Figure 3B), a signature vibrational signal of Cr_2O_3, unambiguously identifies that the chemical nature of the nanoparticles is Cr_2O_3, the reduced product of Cr(VI). In addition, we have also applied EDX to analyze the distributions of elements Cr and Fe on the cell surface. However, for wild type, the Δ*omcA* mutant, and the Δ*mtrC* mutant, we observed Cr but no Fe. Figure 3C shows typical imaging data of wild-type MR-1 after the reduction assay. Under the same background noise level, Cr is clearly observed. For the double mutant Δ*omcA*−Δ*mtrC*, most of the time we observe only smooth cell surfaces, and there is no concentrated Cr or Fe as shown in Figure 3D. On the basis of these observations, we suggest that most of the Cr_2O_3 nanoparticles on the cell surfaces originate from a direct microbial reduction. Our single-cell bioremediation result is consistent with the reported ensemble measurements of a direct microbial reduction mechanism.[12,14]

dx.doi.org/10.1021/la303779y | *Langmuir* 2013, 29, 950−956

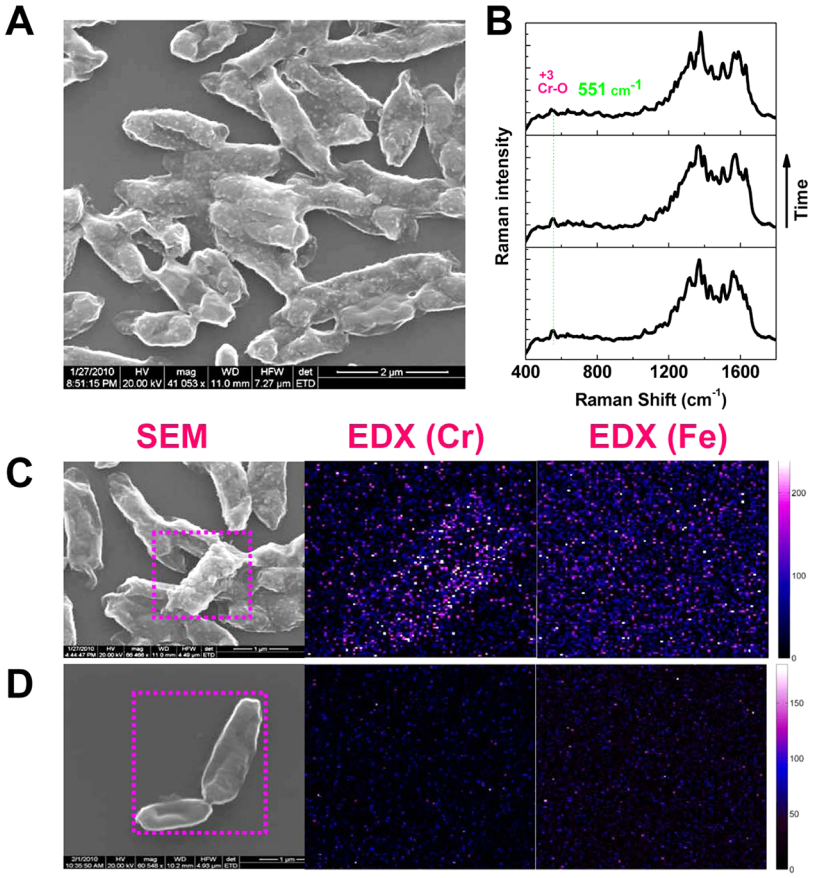

Figure 3. Imaging and spectroscopic characterization of the Cr(VI) reduction with hematite involved. (A) SEM image of wild type MR-1 after hematite-involved Cr(VI) reduction. The appearance of the nanoparticles is obvious on the cell surface. (B) Using SERS, we recorded the specific vibrational mode signature signal of Cr(III)−O in Cr_2O_3 and used it to identify the Cr(III) product redox state. (C) Using EDX, we observed Cr to be concentrated on the cell surface, but no Fe is observed for wild type MR-1. (D) For the double Δ*omcA*−Δ*mtrC* as a reducer, the cell surface is smooth with less possibility of finding the nanoparticles. There is no concentrated Cr or Fe that can be observed using EDX.

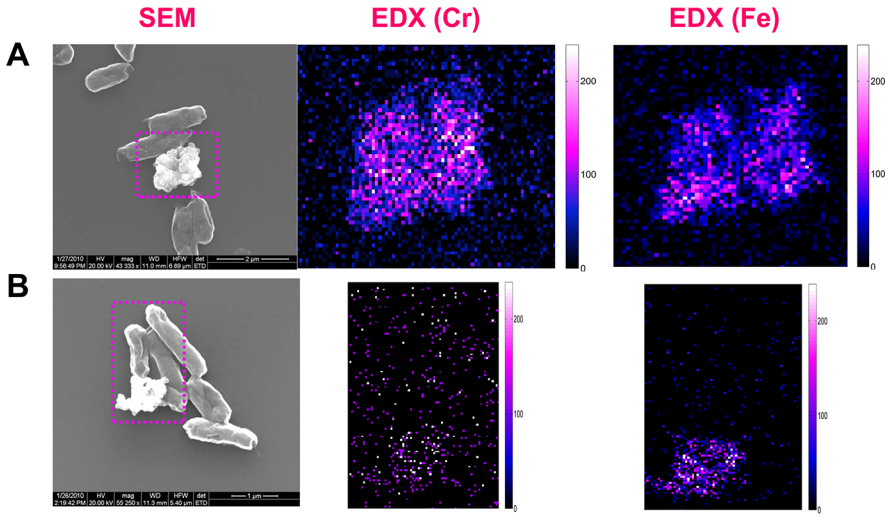

Figure 4. Imaging the chemical compositions of the aggregations after the reduction reaction. (A) Wild-type MR-1 with Cr(VI) and hematite. (B) Mutant Δ*omcA*−Δ*mtrC* with Cr(VI) and hematite.

For the hematite-involved samples, in addition to the observed nanoparticles on cell surfaces, we also observed large aggregations around the cell surfaces. The SEM images are shown in Figure 4. Using EDX characterization, we found concentrated Cr co-localized with Fe in the aggregations for the samples: wild type, mutant Δ*omcA*, and mutant Δ*mtrC*. In contrast, for double mutant Δ*omcA*−Δ*mtrC*, only small concentrations of Cr were observed. Figure 4A,B shows the typical SEM and EDX images for wild type and mutant Δ*omcA*−Δ*mtrC* samples. For a quantitative comparison, we measured the amount of Cr and Fe and calculated the Cr/Fe atomic ratios in the aggregations for all four samples with

dx.doi.org/10.1021/la303779y | *Langmuir* 2013, 29, 950−956

multiple (at least five) independent samplings by using EDX imaging. The Cr/Fe atomic ratios are calculated to be 0.78:1, 0.23:1, 0.32:1, and 0.2:1 for the wild type, single mutant Δ*mtrC*, Δ*omcA*, and double mutant Δ*omcA*-Δ*mtrC* samples, respectively (Figure 5). The heterogeneous distributions

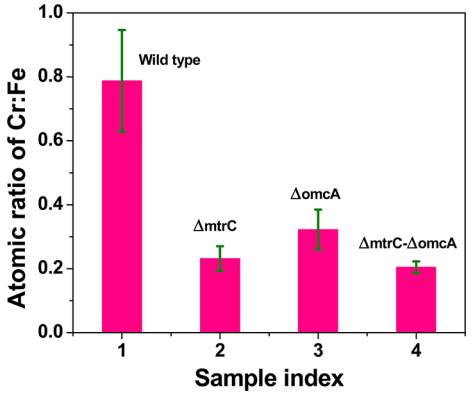

Figure 5. Atomic ratios of Cr/Fe in the aggregations of four control experiments: (left to right) wild type MR-1 with Cr(VI) and hematite, Δ*mtrC* mutant with Cr(VI) and hematite,) Δ*omcA* mutant with Cr(VI) and hematite, and mutant Δ*omcA*−Δ*mtrC* with Cr(VI) and hematite. For each sample, at least five large aggregates were selected for the measurements.

(especially the high concentration for the wild type) of the Cr/Fe atomic ratios imply that the insoluble Cr species (most likely Cr_2O_3) in the hematite aggregations does not originate simply from physical adsorption after direct microbial reduction. In a direct reduction, the ratios should be close to homogeneity after multiple times of independent sampling. Considering that Fe(II) can mediate the electron transfer between MR-1 and Cr(VI),[9,28,29] we suggest that hematite could act as an electron shuttle in our reduction assay experiments. In the Cr(VI) reduction process, in addition to the direct microbial reduction (Figure 6A), MR-1 may first reduce hematite and then the reduced hematite goes on to transfer an electron to the soluble Cr(VI) (Figure 6B). This observation suggests that the direct microbial Cr(VI) reduction and Fe(II)-mediated Cr(VI) reduction mechanisms may coexist in the bioremediation processes. This proposal is also consistent with the previous reports that suggest that several mechanisms may exist in the bacterial metal-reduction process depending on different local environments and conditions.[19]

To reveal the mechanism of the MR-1-involved bioremediation process, several aspects, including the reduction of the protein species, their localization and identification, and the energetics and kinetics of the reduction reactions, still need further specific characterization. The MR-1 genome encodes 42 c-type cytochromes. However, only three of them (OmcA, MtrC, and MtrA) have been demonstrated to be involved in the metal reduction.[19] Except for cytochromes, iron−sulfur proteins and quinones have also been proven to be capable of reducing heavy metals.[19,31,32] We and other groups have demonstrated that the reduction proteins could be localized inside or outside the cell surface or as an external microbial "nanowire" by using Raman spectroscopy and high-resolution topographic imaging techniques.[14,17,19,33] For the energetics and dynamics of the reduction reaction, both theoretical and experimental approaches have been conducted in recent years.[3,10,19] Nevertheless, a real-time quantitative description

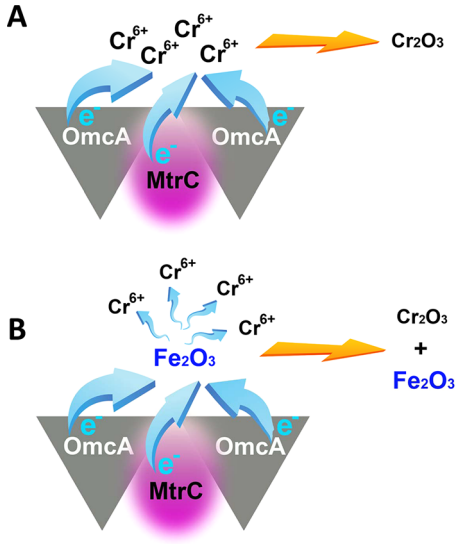

Figure 6. Two mechanisms are proposed to coexist in the in the Cr(VI) reduction process. (A) Direct microbial Cr(VI) reduction. Surface proteins OmcA and MtrC form a functional high-affinity complex in vivo and cooperatively serve as an electron donor. (B) Fe (II)-mediated Cr(VI) reduction. Hematite acts as an electron shuttle between surface proteins and Cr(VI).

of the metal-reducing process could include several important parameters such as the electron-transfer rate of the direct bacterial reduction reaction, the free-energy landscape of the reduction reaction, and the working principles of the electron shuttle in an indirect mechanism.

CONCLUSIONS

We have applied an approach that combines Raman spectroscopy and SEM imaging analyses to characterize the reduction of Cr(VI) to Cr(III) insoluble nanoparticles by c-type cytochromes, MtrC and OmcA, on the bacterial cell surface. Our results demonstrate that (1) MR-1 is capable of reducing toxic Cr(VI) to less-toxic Cr(III)-containing Cr_2O_3 nanoparticle precipitates on the cell surfaces; (2) the cooperation of surface proteins OmcA and MtrC makes the reduction reaction most efficient and the sequence of the reducing reactivity of the MR-1 is wild type > single mutant Δ*mtrC* or Δ*omcA* > double mutant Δ*omcA*−Δ*mtrC*; (3) surface proteins OmcA and MtrC are the terminal reductases of Cr(VI); and (4) direct microbial Cr(VI) reduction and Fe(II)-mediated Cr(VI) reduction mechanisms may coexist in the bioremediation process. These conclusions will advance our understanding of the mechanism and the key parameters in the bioremediation process, such as the localization and identification of the terminal reductases and a mechanical description of the surface chemical reactions. Moreover, these results demonstrate the potential application of SERS in investigating the mechanisms of metal reduction by microbial-surface proteins.

ASSOCIATED CONTENT

Supporting Information

Significance of Raman spectroscopy and methods. SEM image of nanoparticles on the bacterial surface. Control experiments for identification of the heme proteins on the wild-type *Shewanella oneidensis* MR-1 surface using surface-enhanced Raman spectroscopy. This material is available free of charge via the Internet at http://pubs.acs.org.

dx.doi.org/10.1021/la303779y | *Langmuir* 2013, 29, 950−956

AUTHOR INFORMATION

Corresponding Author

*E-mail: hplu@bgsu.edu.

Notes

The authors declare no competing financial interest.

ACKNOWLEDGMENTS

This work was supported by NIH NIEHS (5R01ES017070-03).

REFERENCES

(1) (a) Imam Khasim, D.; Nanda Kumar, N. V.; Hussain, R. C. Enviromental Contamination of Chromium in Agricultural and Animal Products Near a Chromate Industry. *Bull. Environ. Contam. Toxicol.* **1989**, *43*, 742−746. (b) Lovley, D. R. Dissimilatory Metal Reduction. *Annu. Rev. Microbiol.* **1993**, *47*, 263−90.

(2) (a) Yeates, G. W.; Orchard, V. A.; Speir, T. W.; Hunt, J. W.; Hermans, M. C. C. Impact of Pasture Contamination by Copper, Chromium, Arsenic Timber Preservative on Soil Biological Activity. *Biol. Fertil. Soils* **1994**, *18*, 200−208. (b) Chen, J. M.; Hao, O. J. Microbial Chromium(VI) Reduction. *Crit. Rev. Environ. Sci. Technol.* **1998**, *28*, 219−251.

(3) Viamajala, S.; Peyton, B.; Petersen, J. Modeling Chromate Reduction in *Shewanella oneidensis* MR-1: Development of a Novel Dual-Enzyme Kinetic Model. *Biotechnol. Bioeng.* **2003**, *83*, 790−797.

(4) Bencheikh-Latmani, R.; Obraztsova, A.; Mackey, M.; Ellisman, M.; Tebo, B. Toxicity of Cr(III) to *Shewanella sp*. Strain MR-4 during CR(VI) Reduction. *Environ. Sci. Technol.* **2007**, *41*, 214−220.

(5) Bencheikh-Latmani, R.; Williams, S.; Haucke, L.; Criddle, C.; Wu, L.; Zhou, J.; Tebo, B. Global Transcriptional Profiling of *Shewanella oneidensis* MR-1 during Cr(VI) and U(VI) Reduction. *Appl. Environ. Microbiol.* **2005**, *71*, 7453−7460.

(6) Daulton, T.; Little, B.; Lowe, K.; Jones-Meehan, J. Electron Energy Loss Spectroscopy Techniques for the Study of Microbial Chromium(VI) Reduction. *J. Microbiol. Methods* **2002**, *50*, 39−54.

(7) Wang, Y.-T. Microbial Reduction of Chromate. In *Environmental Microbe-Metal Interactions*; Lovley, D. R., Ed.; ASM Press: Washington D.C., 2000; pp 225−235.

(8) Lovley, D. Dissimilatory Metal Reduction. *Annu. Rev. Microbio.* **1993**, *47*, 263−290.

(9) (a) Wielinga, B.; Mizuba, M. M.; Hansel, C. M.; Fendorf, S. Iron Promoted Reduction of Chromate by Dissimilatory Iron-Reducing Bacteria. *Environ. Sci. Technol.* **2001**, *35*, 522−527. (b) Fendorf, S.; Wielinga, B. W.; Hansel, C. M. Chromium Transformations in Natural Environments: The Role of Biological and Abiological Processes in Chromium(VI) Reduction. *Int. Geol. Rev.* **2000**, *42*, 691−701.

(10) Belchik, S. M.; Kennedy, D. W.; Dohnalkova, A. C.; Wang, Y.; Sevinc, P. C.; Wu, H.; Lin, Y.; Lu, H. P.; Fredrickson, J. K.; Shi, L. Extracellular Reduction of Hexavalent Chromium by Cytochromes MtrC and OmcA of *Shewanella oneidensis* MR-1. *Appl. Environ. Microb.* **2011**, *77*, 4035−4041.

(11) Middleton, S.; Latmani, R.; Mackey, M.; Ellisman, M.; Tebo, B. M.; Criddle, C. S. Cometabolism of Cr(VI) by *Shewanella oneidensis* MR-1 Produces Cell-Associated Reduced Chromium and Inhibits Growth. *Biotechnol. Bioeng.* **2003**, *83*, 627−637.

(12) Myers, C. R.; Carstens, B. P.; Antholine, W. E.; Myers, J. M. Chromium(VI) Reductase Activity Is Associated with the Cytoplasmic Membrane of Anaerobically Grown *Shewanella putrefaciens* MR-1. *J. Appl. Microbiol.* **2000**, *88*, 98−106.

(13) Neal, A.; Lowe, K.; Daulton, T.; Jones-Meehan, J.; Little, B. Oxidation State of Chromium Associated with Cell Surfaces of *Shewanella oneidensis* during Chromate Reduction. *Appl. Surf. Sci.* **2002**, *202*, 150−159.

(14) Ravindranath, S. P.; Henne, K. L.; Thompson, D. K.; Irudayaraj, J. Raman Chemical Imagining of Chromate Reduction Sites in a Single Bacterium using Intracellularly Grown Gold Nanoislands. *ACS Nano* **2011**, *5*, 4729−4736.

(15) (a) Jarvis, R. M.; Goodacre, R. Discrimination of Bacteria Using Surface-Enhanced Raman Spectroscopy. *Anal. Chem.* **2004**, *76*, 40−47. (b) Premasiri, W. R.; Gebregziabher, Y.; Ziegler, L. D. On the Difference Between Surface-Enhanced Raman Scattering (SERS) Spectra of Cell Growth Media and Whole Bacterial Cells. *Appl. Spectrosc.* **2011**, *65*, 493−499. (c) Colthup, N.; Daly, L.; Wiberley, S. *Introduction to Infrared and Raman Spectroscopy*; Academic Press: New York, 1990.

(16) Stiles, P. L.; Dieringer, J. A.; Shah, N. C.; Van Duyne, R. P. Surface-Enhanced Raman Spectroscopy. *Annu. Rev. Anal. Chem.* **2008**, *1*, 601−626.

(17) Biju, V.; Pan, D.; Gorby, Y. A.; Fredrickson, J.; McLean, J.; Saffarini, D.; Lu, H. P. Combined Spectroscopic and Topographic Characterization of Nanoscale Domains and Their Distrubitions of a Redox Protein on Bacterial Cell Surfaces. *Langmuir* **2007**, *23*, 1333−1338.

(18) Shi, L.; Chen, B.; Wang, Z.; Elias, D.; Mayer, M.; Gorby, Y. A.; Ni, S.; Lower, B. H.; Kennedy, D. W.; Wunschel, D. S.; Mottaz, H. M.; Marshall, M. J.; Hill, E. A.; Beliaev, A. S.; Zachara, J. M.; Frederickson, J. K.; Squier, T. C. Isolation of a High-Affinity Functional Protein Complex between OmcA and MtrC: Two Outer Membrane Decaheme c-Type Cytochromes of *Shewanella oneidensis* MR-1. *J. Bacteriol.* **2006**, *188*, 4705−4714.

(19) Meitl, L. A.; Eggleston, C.; Colberg, P. J. S.; Khare, N.; Reardon, C.; Shi, L. Electrochemical Interaction of *Shewanella oneidensis* MR-1 and Its Outer Membrane Cytochromes OmcA and MtrC with Hematite Electrodes. *Geochim. Cosmochim. Acta* **2009**, *73*, 5292−5307.

(20) Beliaev, A. S.; Saffarini, D. A.; McLaughlin, J. L.; Hunnicutt, D. MtrC, an Outer Membrane Decahaem c Cytochrome Required for Metal Reduction in *Shewanella putrefaciens* MR-1. *Mol. Microbiol.* **2001**, *39*, 722−730.

(21) Myers, J. M.; Myers, C. R. Genetic Complementation of an Outer Membrane Cytochrome *omcB* Mutant of *Shewanella putrefaciens* MR-1 Requires *omcB* Plus Downstream DNA. *Appl. Environ. Microbiol.* **2002**, *68*, 2781−2793.

(22) Myers, J. M.; Myers, C. R. Role for Outer Membrane Cytochromes OmcA and OmcB of *Shewanella putrefaciens* MR-1 in Reduction of Manganese Dioxide. *Appl. Environ. Microbiol.* **2001**, *67*, 260−269.

(23) Xiong, Y.; Shi, L.; Chen, B.; Mayer, M. U.; Lower, B. H.; Londer, Y.; Bose, S.; Hochella, M. F.; Fredrickson, J. K.; Squier, T. C. High-Affinity Binding and Direct Electron Transfer to Solid Metals by the *Shewanella oneidensis* MR-1 Outer Membrane c-type Cytochrome OmcA. *J. Am. Chem. Soc.* **2006**, *128*, 13978−13979.

(24) Feng, M.; Tachikawa, H. Surface-Enhanced Resonance Raman Spectroscopic Characterization of the Protein Native Structure. *J. Am. Chem. Soc.* **2008**, *130*, 7443−7448.

(25) De Groot, J.; Hester, R. E. Surface-Enhanced Resonance Raman Spectroscopy of Oxyhemoglobin Adsorbed onto Colloidal Silver. *J. Phys. Chem.* **1987**, *91*, 1693−1696.

(26) Mougin, J.; Rosman, N.; Lucazeau, G.; Galerie, A. In Situ Raman Monitoring of Chromium Oxide Scale Growth for Stress Determination. *J. Raman. Spectrosc.* **2001**, *32*, 739−744.

(27) (a) Yu, T.; Shen, Z. X.; He, J.; Sun, W. X.; Tang, S. H.; Lin, J. Y. Phase Control of Chromium Oxide in Selective Microregions by Laser Annealing. *J. Appl. Phys.* **2003**, *93*, 3951−3953. (b) McCreery, R. L.; Packard, R. T. Raman Monitoring of Dynamic Electrochemical Events. *Anal. Chem.* **1989**, *61*, 775A.

(28) Caccavo, F., Jr.; Ramsing, N. B.; Costerton, J. W. Morphological and Metabolic Responses to Starvation by the Dissimilatory Metal-Reducing Bacterium *Shewanella alga* BrY. *Appl. Environ. Microbiol.* **1996**, *62*, 4678−4682.

(29) Nyman, J. L.; Caccavo, F., Jr.; Cunningham, A. B.; Gerlach, R. Metal-Reducing Bacteria Facilitate the Geochemical Elemination of Cr(VI) from Contaminated Water. *Biorem. J.* **2002**, *6*, 39−55.

(30) Bose, S.; Hochella, M. F., Jr.; Gorby, Y. A.; Kennedy, D. W.; McCready, D. E.; Madden, A. S.; Lower, B. H. Bioreduction of Hematite Nanoparticles by the Dissimilatory Iron Reducing Bacterium

Shewanella oneidensis MR-1. *Geochim. Cosmochim. Acta* **2009**, *73*, 962−976.
(31) Richardson, D. J. Bacterial Resperation: A Flexible Process for a Changing Enviroment. *Microbiology* **2000**, *146*, 551−571.
(32) Giometti, C. In *Microbial Proteomics: Functional Biology of Whole Organisms*; Humphery-Smith, I., Hecker, M., Eds.; Methods of Biochemical Analysis; Wiley-Liss: Hoboken, NJ, 2006; Vol. *49*, pp 97−111.
(33) Marshall, M. J.; Beliaev, A. S.; Dohnalkova, A. C.; Kennedy, D. W.; Shi, L.; Wang, Z.; Boyanov, M. I.; Lai, B.; Kemner, K. M.; McLean, J. S.; Reed, S. B.; Culley, D. E.; Bailey, V. L.; Simonson, C. J.; Saffarini, D. A.; Romine, M. F.; Zachara, J. M.; Fredrickson, J. K. c-Type Cytochrome-Dependent Formation of U(IV) Nanoparticles by *Shewanella oneidensis*. *PLoS Biol.* **2006**, *4*, 1324.